Design of dynamically optimal spline motion inputs: Experimental results

Jan De Caigny, Bram Demeulenaere, Jan Swevers and Joris De Schutter

Abstract— **This work considers the design of point-to-point input trajectories for flexible motion systems. The objective is to excite the system's dynamics as little as possible so as to reduce residual vibration and settling time. Simulation and experimental results of a recently developed optimization framework for polynomial splines are presented. This framework is capable of automatically selecting the optimal number and location of the knots of the polynomial spline and allows input constraints and robustness against parametric uncertainty and unmodeled dynamics to be included during the design. The obtained results are compared to two literature benchmark methods.**

I. INTRODUCTION

Trajectory design for flexible motion systems, for example cam and servo motor systems, aims at shaping the system input such that the output behaves in a satisfactory manner. Several approaches have been presented in literature, which can be categorized roughly in two main classes: filter design and input design [2]. Filter design (see [7, 8] among others) is the more general technique since any motion reference can be convolved with the designed filter to create the appropriate system input, whereas input design methods (see e.g. [1, 4, 5, 9]) need to determine a new system input for every new motion.

This paper discusses the application of the optimization framework for designing polynomial spline inputs developed by Demeulenaere *et al.* in [2] on a two Degree-of-Freedom (2-DOF) flexible motion system to achieve fast point-to-point motions with reduced residual vibrations. Both simulation and experimental results are presented. The results obtained with the optimal polynomial spline trajectories are compared to two benchmark methods from the literature. The first benchmark is input shaping, a filter design method proposed by Singer and Seering [7]. The second benchmark is an input design method based on Bernstein-Bézier harmonic curves developed by Srinivasan and Ge [9].

The paper is organized as follows. Sec. II gives a short overview of the optimization framework for polynomial splines. Next, residual vibrations of a flexible motion system for a given point-to-point input are quantified in Sec. III, after which Sec. IV presents the application. The test-setup is introduced and the results of the two considered benchmark methods and the spline optimization framework are compared. Sec. V concludes the paper.

II. BASIC SPLINE OPTIMIZATION FRAMEWORK

This section gives a short overview of the optimization framework for polynomial splines presented in [2]. First, the terminology is introduced and a definition is given for polynomial splines.

A motion trajectory $s(t)$, defined on a finite time interval $[0, t_e]$, is a polynomial *spline* of *degree* $k \geq 0$, having as *knots* the strictly[1] increasing sequence t_i, $i = 0, \ldots, g+1$ ($t_0 = 0$, $t_{g+1} = t_e$) if [3]:

- $s(t)$ is a polynomial of degree $\leq k$ on each knot interval $[t_i, t_{i+1}]$:
$$s_{[t_i, t_{i+1}]} \in \mathscr{P}_k, \ i = 0, \ldots, g. \quad (1)$$

- $s(t)$ and its derivatives up to order $k-1$ are continuous on $[0, t_e]$:
$$s(t) \in \mathscr{C}^{k-1}[0, t_e]. \quad (2)$$

A knot is called *active* if the kth-order derivative of $s(t)$ features a discontinuous jump at t_i (as allowed by the previous definition). The knots t_i, for $i = 1 \ldots g$ are the g *internal* knots.

Several approaches exist to optimize polynomial splines. If the degree k, the number g and the location of the internal knots are given, it suffices to find the coefficients of the polynomials $s_{[t_i, t_{i+1}]}$ on each knot interval. Depending on the optimization criterion this is a rather straightforward problem. In contrast, the problem becomes a nonlinear optimization problem with a lot of local optima when only the degree k and the number of knots g are given, but not their location. In the approach presented in [2], this problem is avoided by choosing a very fine, equidistant sequence of *possible* knots,

$$t_i = i \cdot \Delta t, \ i = 0, \ldots, g+1 \text{ where } \Delta t = \frac{t_e}{g+1}$$

with typical values of $g = 500 \ldots 2000$.

The consequence of this indirect (basis pursuit) approach is that the only variables that need to be determined are the coefficients of the polynomials on each knot interval. Choosing affine cost functions and constraints the optimization results in a medium-scale (typically with a few thousands of variables) sparse linear program that can be solved very efficiently with a guarantee of optimality. Moreover, by controlling the smoothness of the spline, i.e. the peak values of the higher derivatives, the number of *active* knots

---

[1]If the knot sequence is increasing, but not strictly increasing (that is, coincident knots are present), the continuity condition (2) has to be relaxed: if $t_{i-1} < t_i = \cdots = t_{i+l} < t_{i+l+1}$, $s(t)$ only has continuous derivatives up to order $k-1-l$ at $t = t_i$ ($l \leq k$).

Mechanical Engineering Department, Katholieke Universiteit Leuven, Celestijnenlaan 300B, B-3001 Leuven, Belgium
`jan.decaigny@mech.kuleuven.be`

"chosen" by solving the optimization problem is often very small yielding a compact representation of the spline.

Some technical issues are discussed now. The interested reader is referred to [2] for further details. Since the polynomial spline is found as the numerical solution of an optimization problem, a general parameterization is required to guarantee that

$$s(t) \in \mathscr{C}^{k-1}_{[0,t_e]} \text{ and } s(t) \notin \mathscr{C}^{k}_{[0,t_e]}.$$

Therefore the $k-1$st-order derivative of $s(t)$, denoted here as $s^{(k-1)}(t)$, is parameterized as a piecewise-linear, continuous function. This is guaranteed by using B-splines (see [3]) of order 2, denoted here as $\beta_i(t)$ for $i = 0,\dots,g+1$, as base functions for $s^{(k-1)}(t)$:

$$s^{(k-1)}(t) = \sum_{i=0}^{g+1} b_i \cdot \beta_i(t) \quad \text{with} \quad b_i = s^{(k-1)}(t_i).$$

This parameterization becomes more general as $g \to \infty$, i.e. as $\Delta t \to 0$. The spline $s(t)$ is obtained by integrating $s^{(k-1)}(t)$ $k-1$ times, thus introducing $k-1$ unknown integration constants as variables in the optimization problem. This results in a parameterization for $s(t)$ which is linear in $g+k+3$ optimization variables: the $g+2$ values $s^{(k-1)}(t_i)$, for $i = 0,\dots,g+1$ and the $k+1$ integration constants.

The *basic* program to optimize $s(t)$ aims at maximizing the smoothness of the polynomial spline, given linear constraints on its position, velocity and higher derivatives. Smoothness is generally associated with peak values of the higher derivatives of $s(t)$ and in the optimization framework, it is quantified by two characteristics of the spline: the ∞-norm of the kth-order derivative and the 1-norm of $k+1$st-order derivative. These characteristics are affine functions of the optimization variables, as explained in [2]. Therefore, using these characteristics as cost function results in a linear program.

This *basic* optimization problem can be extended to include bounds on the residual vibration of a flexible motion system under parametric and dynamic system uncertainty (see Sec. III). This will come at the cost of a less smooth spline.

III. RESIDUAL VIBRATION OF A FLEXIBLE SYSTEM

A one Degree-of-Freedom (1-DOF) system typically has the following equation of motion

$$\ddot{y}(t) + 2\zeta\omega_0\,\dot{y}(t) + \omega_0^2\,y(t) = \omega_0^2\,u(t), \tag{3}$$

with ω_0 the undamped resonance frequency of the system and ζ the corresponding damping ratio. For such a system, Fig. 1 shows the response $y(t)$ (dash-dotted) for a fast point-to-point motion input $u(t)$ (solid) with a rise portion ($0 \le t \le t_e$) and a dwell portion $t > t_e$. The notion of a *"fast"* or *"slow"* input is quantified by the dimensionless ratio

$$\lambda = \frac{t_e}{t_0} = t_e \cdot \frac{\omega_0}{2\pi} \ [-], \tag{4}$$

where t_e is the duration of the rise portion of the input trajectory and

$$t_0 = \frac{2\pi}{\omega_0} \ [s] \tag{5}$$

the natural period of the system. The ratio λ represents the dimensionless undamped resonance frequency and can be interpreted as the number of periods, corresponding to the undamped resonance frequency ω_0, that fits into the time interval $[0,t_e]$. In general, values of λ smaller than 10 are considered to be fast.
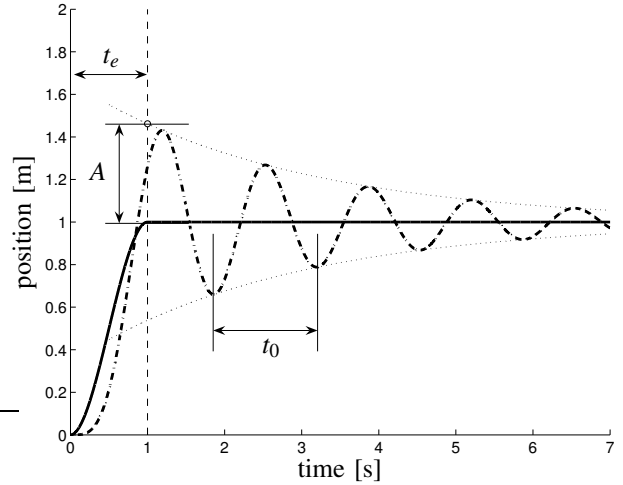

Fig. 1. System response (dash-dotted) for a fast point-to-point motion input trajectory (solid).

After the rise portion of the input, the system response is a free oscillation with viscous damping. A good measure of the amplitude of the residual dwell vibration is the amplitude A of its exponential envelope at $t = t_e$

$$A = \frac{\sqrt{y(t_e)^2 + 2\zeta y(t_e)(\dot{y}(t_e)/\omega_0) + (\dot{y}(t_e)/\omega_0)^2}}{\sqrt{1-\zeta^2}} \ [m]. \tag{6}$$

Both the exponential envelope (dotted) and the amplitude of the residual vibration A are indicated in Fig. 1. From Eq. (6) it is clear that for a 1-DOF system the amplitude of the residual vibration is a function of the system characteristics ω_0 and ζ and of the position and velocity of the output at time t_e. Given the linear system dynamics (3), the output at time t_e is a linear function of the input $u(t)$, for $0 \le t \le t_e$. Therefore the ratio λ, the damping ζ and a given point-to-point input trajectory $u(t)$ with duration t_e completely determine A for a 1-DOF system. From (6) it is clear that A^2 is a quadratic function of the output position and velocity and since these are linear in the input $u(t)$, A^2 is a quadratic function of the input. As explained in the previous sections, the optimization framework uses a linear parameterization for the input. Consequently, A^2 constitutes a quadratic function in the spline parameters.

All concepts introduced above can be extended to multiple Degree-of-Freedom flexible systems. Multiple DOF systems can be characterized by multiple resonance frequencies ω_i

and corresponding damping ratios ζ_i, for $i = 0, \ldots, N$, with $N + 1$ the number of DOFs in the model. Similarly as for 1-DOF systems, dimensionless resonance frequencies $\lambda_i = t_e/t_i$, with $t_i = \frac{2\pi}{\omega_i}$ can be defined. If the resonance frequencies are sorted such that

$$\omega_0 \leq \ldots \leq \omega_{i-1} \leq \omega_i \leq \omega_{i+1} \leq \ldots \leq \omega_N,$$

the corresponding λ_i are sorted as well

$$\lambda_0 \leq \ldots \leq \lambda_{i-1} \leq \lambda_i \leq \lambda_{i+1} \leq \ldots \leq \lambda_N.$$

For a given multiple DOF flexible system and a given input, perfect nominal performance is achieved if, in the absence of any uncertainty or modeling error, the amplitude of the residual vibration is zero. However, most systems are not perfectly known and therefore the input trajectories have to be robust against 1) small perturbations on the system parameters ω_i and ζ_i, 2) small perturbations on the duration of the rise portion t_e and 3) unmodeled higher dynamics. To guarantee 1) and 2) the amplitude of the residual vibration A has to be small for a range of λ-values around the nominal value of each λ_i. To guarantee 3) A has to be sufficiently small for all values of $\lambda \geq \lambda_N$. Most methods published in the literature demand perfect nominal performance and add robustness in a second step. In this paper, however, it will be shown that relaxing the perfect nominal performance requirement, provides additional design freedom to improve robustness.

As mentioned before, the test-setup is a 2-DOF system, so for a given input with duration t_e it can be represented by 2 dimensionless resonances λ_0 and λ_1 with the corresponding damping ratios ζ_0 and ζ_1. However, one of the goals of this case-study is to check the robustness of the different methods against unmodeled higher dynamics. Therefore, during the design of the inputs, only information about the first resonance frequency (λ_0, ζ_0) is used.

Both benchmark methods use a local sensitivity approach to include robustness, i.e. robustness is obtained by setting the first-order sensitivity

$$\left.\frac{\partial A}{\partial \lambda}\right|_{\lambda = \lambda_0} = 0. \tag{7}$$

Higher-order robustness can be included by setting the higher derivatives of A with respect to λ to zero as well.

The spline optimization framework uses a global sensitivity approach by imposing the following inequality constraints

$$A(\lambda) \leq \varepsilon, \text{ for } \lambda \in \Lambda = [\underline{\lambda}, \bar{\lambda}], \text{ with } \lambda_0 \in \Lambda. \tag{8}$$

Sec. IV-C explains how this upper bound on the amplitude of the residual vibration is imposed in the optimization framework presented in Sec. II. But first, the test-setup is introduced in Sec. IV-A and the benchmark methods from the literature are presented in Sec. IV-B.

IV. APPLICATION: FLEXIBLE MOTION SYSTEM

A. Two Degree-Of-Freedom Test-Setup

The test-setup considered is a 2-DOF mass-spring-damper system. Fig. 2 presents a picture and a schematic drawing of
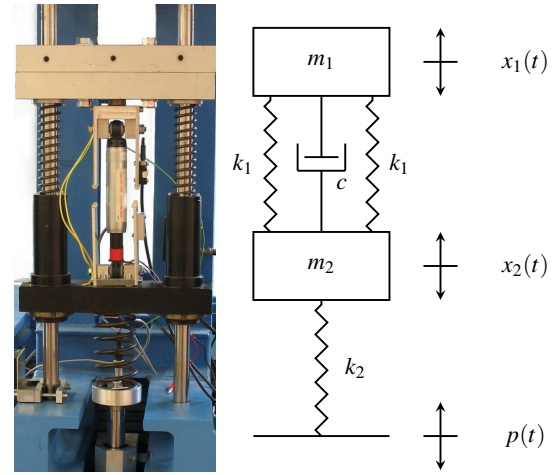

Fig. 2. Picture and schematic drawing of the test-setup.

the setup. The system is excited by a hydraulic piston whose position is indicated by $p(t)$. This piston is driven by a servo valve which is controlled using a PID-controller to track a reference position $r(t)$ as shown in Fig. 3. The bandwidth of the closed-loop $P(s)/R(s)$ is 22Hz. The position of the upper mass $x_1(t)$ is chosen as the system's output. The dynamics of the system come from three springs; two with stiffness k_1 and one with stiffness k_2. The damping in the system is represented by the dashpot c.
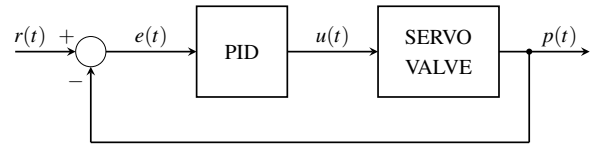

Fig. 3. Control configuration for the hydraulic piston.

Frequency response functions (FRFs) of the system are measured using multisine excitation with a frequency content between 0.1Hz and 10Hz and a sample frequency of 2kHz. Statespace models are fitted on these FRFs using a nonlinear least-squares frequency identification method [6]. Fig. 4 shows two measured FRFs and the two corresponding identified models. The blue curve ($+$ marks) shows the FRF relating $r(t)$ to $x_1(t)$. The red line indicates the corresponding identified model $X_1(s)/R(s)$. The green curve ($*$ marks) shows the FRF relating $p(t)$ to $x_1(t)$. The black line indicates the corresponding identified model $X_1(s)/P(s)$. Both $X_1(s)/R(s)$ and $X_1(s)/P(s)$ clearly show a first resonance at

$$\omega_0 = 2.6205 \cdot 2\pi \text{ rad/s with } \zeta_0 = 1.57\%$$

and a second resonance at

$$\omega_1 = 7.7926 \cdot 2\pi \text{ rad/s with } \zeta_1 = 2.93\%.$$

Notice that there is little or no difference between the two FRFs at low frequencies. However, at higher frequencies a clear phase shift is noticeable which can be explained by the limited bandwidth of the piston position PID-controller.
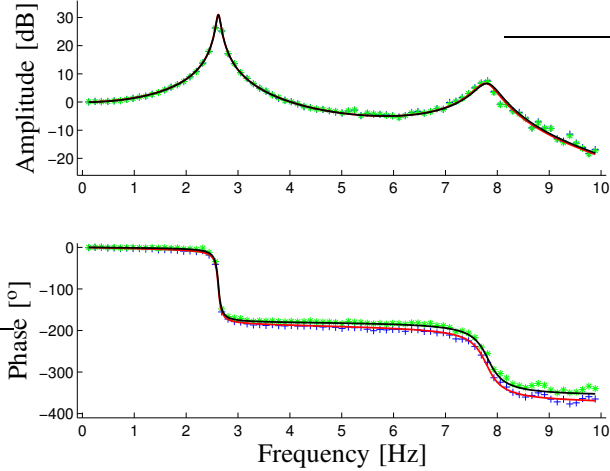
Fig. 4. Measured FRFs and identified models relating $x_1(t)$ to $p(t)$ and $r(t)$.

Fig. 5. Original input, input shaping filter and the resulting shaped input.

For the benchmark methods as well as for the spline design the nominal λ is chosen to be 2, which means that the inputs for this application have a total duration

$$t_e = \lambda \frac{2\pi}{\omega_0} = 2 \frac{2\pi}{2.6205 \cdot 2\pi} = 0.7632 \text{s}.$$

B. Benchmark Results

i. Input shaping

Input shaping is a well-known method to analytically calculate finite impulse response (FIR) filters, consisting of a series of positive impulses, that are able to reduce the system's residual vibration. It is an elegant, widely spread and straightforward procedure that is capable of including robustness against perturbations in both λ and ζ. A drawback is that a short move-time penalty is incurred (the duration of the filter).

For the considered application a filter was calculated, using the procedure developed in [7], with perfect nominal performance and first-order robustness. The resulting filter consists of only 3 impulses and has a duration of 0.3816s (see Fig. 5 b). By convolving a ramp input (Fig. 5 a) with a duration of 0.3816s as well, a shaped input (Fig. 5 c) is obtained with a total duration of $t_e = 0.7632$s which corresponds to $\lambda = 2$. This ramp input can be interpreted as a velocity pulse of 0.3816s, which is similar to the input originally used in [7]. Notice that by choosing a ramp input as the original input, the obtained shaped input has a non-zero velocity at the start and the end of the trajectory.

ii. Bernstein-Bézier Harmonic Curves

Bernstein-Bézier harmonic curves constitute an interesting family of curves since they have a low frequency content that is explicitly known. Following the procedure presented in [9], in a first step, a Bernstein-Bézier harmonic is calculated analytically for the desired output, based on the requirements of perfect nominal performance and first-order robustness. In a second step the corresponding Bernstein-Bézier harmonic
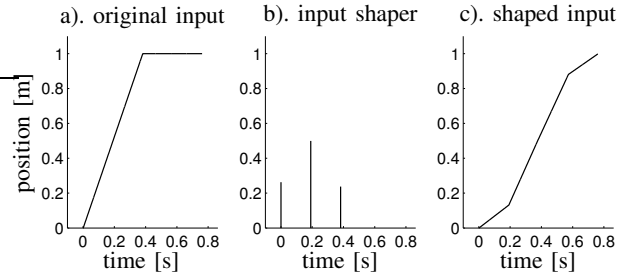
input, necessary to obtain the desired output, is calculated analytically using the inverse dynamics of the system. The calculation of the desired output in the first step can become time-consuming for higher-order robustness. Both the desired output (solid) and the corresponding calculated input (dash-dotted) are shown in Fig. 6. The desired output clearly has zero velocity at the boundaries. This however, is not the case for the calculated input, which starts and ends with a nonzero velocity.
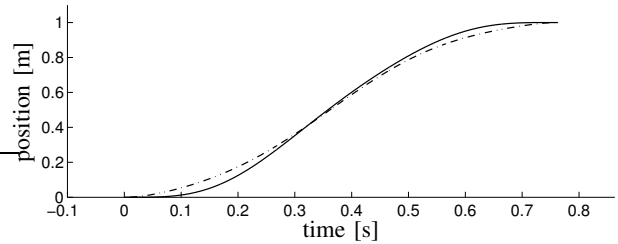

Fig. 6. Desired output (solid) and calculated input (dash-dotted) using Bernstein-Bézier harmonic curves.

C. Polynomial Spline Results

A polynomial spline with degree $k = 5$ is optimized considering the following constraint and goal function.

- Robustness against uncertainty on λ_0 is included here by choosing a set of M values $\tilde{\lambda}_j$ from the uncertain set $\Lambda = [\underline{\lambda}, \bar{\lambda}]$, constructing their corresponding models (3) and imposing inequality constraints on the residual vibration for these models. As explained in [2], the constraint $A(\tilde{\lambda}_j)^2 \leq \varepsilon^2$ which is quadratic in the spline parameterization, can be replaced by a conservative set of four linear constraints for every $\tilde{\lambda}_j$.
- The cost function is the ∞-norm of the kth-order derivative. Minimizing this cost function yields that extreme values of the higher derivatives are clipped off.
- Since both benchmark methods allow a velocity discontinuity at the start $t = 0$ and end $t = t_e$ of the trajectory, this design freedom is given to the spline optimization framework as well. This, however, is rather counterintuitive since the imposed continuity of the spline for $0 < t < t_e$ is higher.

Fig. 7 shows the position, velocity and higher derivatives of the polynomial spline that was found using the following

settings: number of internal knots $g = 511$, total spline duration $t_e = 0.7632$s and bound on the residual vibrations $\varepsilon = 0.75\%$ for $\tilde{\lambda}_j \in [1.7 : 0.01 : 3]$ ($M = 131$). The resulting spline clearly shows only 4 *active* internal knots, although 511 possible knots were provided and the associated cost $||s^{(5)}(t)||_\infty = 1.0493e^4 [m/s^5]$ as can be seen from Fig. 7 f. Although the optimization framework allows to include robustness against unmodeled higher dynamics, this is not included in the design of this spline. The results shown in the following section motivate this choice.
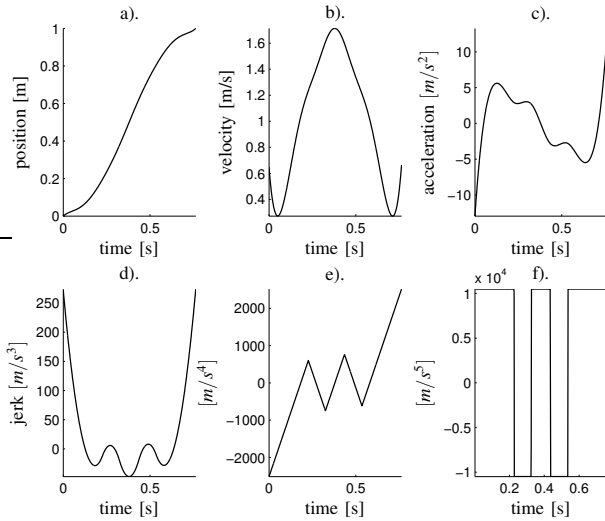
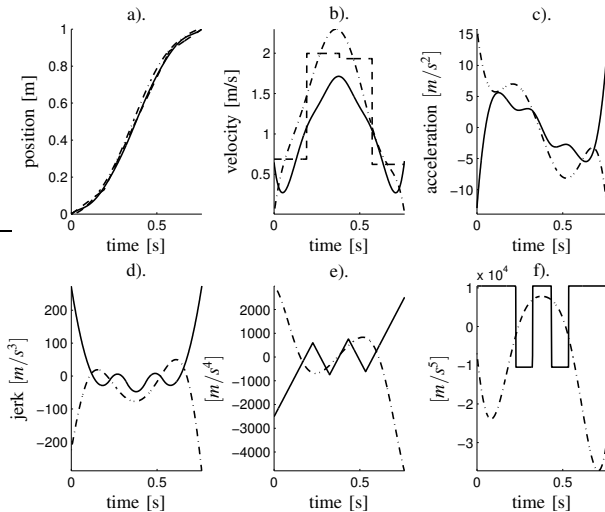Fig. 7. Polynomial spline and its derivatives.

D. Comparison

Fig. 8. Position, velocity and higher derivatives of the polynomial spline (solid), the shaped input (dashed) and the Bernstein-Bézier harmonic curve (dash-dotted).

Fig. 8 shows the position, the velocity and the higher derivatives of the three inputs derived in Sec. IV-B and IV-C. The shaped input (dashed) has a piecewise-linear

continuous position and discontinuous jumps in its velocity (Fig. 8 b). Therefore, higher derivatives are not shown for the shaped input. The polynomial spline (solid) has degree $k = 5$, which means the derivative of the jerk is piecewise-linear continuous and the fifth-order derivative shows discontinuous jumps (Fig. 8 f). Since the Bernstein-Bézier harmonic curves can be represented by a finite sum of sines and cosines, they can be derived infinitely many times. Compared to the shaped input and the Bernstein-Bézier harmonic, the polynomial spline shows the smallest ∞-norm of the velocity. The same holds when comparing the higher derivatives of the Bernstein-Bézier harmonic and the polynomial spline. Lower peak values for the derivatives are obviously beneficial for the system.

The goal of the case-study is to measure the amplitude of the residual vibration as a function of λ for the three inputs shown in Fig. 8. To do so, the following approach is adopted. Since the test-setup has fixed resonance frequencies, the only freedom left to influence λ is the duration t_e of the input. Thus, instead of varying the system, the input is stretched or compressed in time, as shown in Fig. 9 for the polynomial spline input and three different values of $t_e = [0.6487, 0.7632, 1.1448]$s corresponding to three different values of $\lambda_1 = [1.7, 2, 3]$.
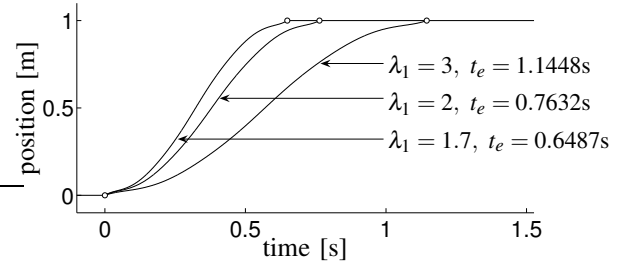

Fig. 9. Polynomial spline input compressed/stretched for $\lambda_1 = [1.7, 2, 3]$

Figs. 10, 11 and 12 show the amplitudes of the residual vibrations for values of $\lambda \in [1.25, 4]$, for the three inputs designed in the previous section. Simulation results based on the 1-DOF and the 2-DOF model and experimental results on the test-setup are compared. Five conclusions can be drawn. 1) The two benchmark results have perfect nominal performance, i.e. the amplitude of the residual vibration is zero for $\lambda = 2$. As this was not imposed in the polynomial spline optimization, this input doesn't yield perfect nominal performance. 2) The polynomial spline input clearly outperforms the two benchmark methods. The measured amplitude of the residual vibrations is below 0.75% for a range of $\lambda \in [1.7, 4]$ which is clearly larger than the robustness range of the other methods. So the fact that perfect nominal performance is not required in the polynomial spline design is largely exploited to suppress the residual vibrations over a wide λ-range. 3) The experimental results correspond quite well to the simulation results, indicating that the used models are accurate representations of the actual test-setup. 4) The 1- and 2-DOF models produce very similar results

for all designed inputs indicating that for this application, the unmodeled second resonance frequency is (almost) not excited by any of the three inputs. This can be explained by the fact that due to the higher damping of the second mode the peak of the FRF at the second resonance frequency lies over 20dB below the peak at the first resonance frequency (see Fig. 4). 5) For the two benchmark methods, robustness was imposed using a local sensitivity approach. Comparing Figs. 10 and 11 shows that in a small range around the nominal λ-value, the shaped input is more robust than the Bernstein-Bézier input. For higher values $\lambda \geq 2.6$, however, the Bernstein-Bézier input yields lower residual vibrations.
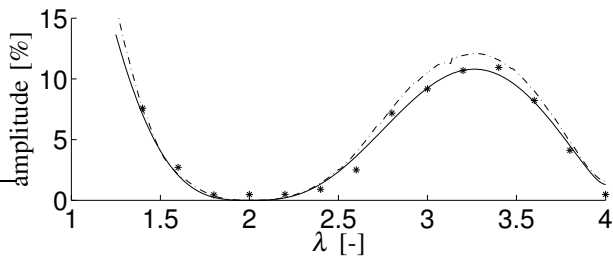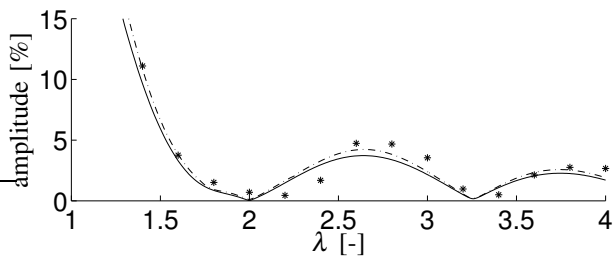

Fig. 10. Amplitude of the residual vibration for $\lambda \in [1.25, 4]$: Comparison of 1-DOF (solid), 2-DOF model (dash-dotted) simulation and experimental ($*$ marks) results for the shaped input.
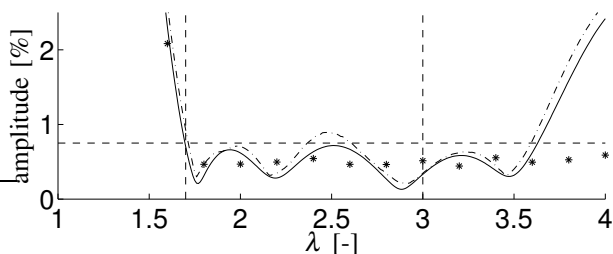

Fig. 11. Amplitude of the residual vibration for $\lambda \in [1.25, 4]$: Comparison of 1-DOF (solid), 2-DOF model (dash-dotted) simulation and experimental ($*$ marks) results for the Bernstein-Bézier harmonic input.

Fig. 12. Amplitude of the residual vibration for $\lambda \in [1.25, 4]$: Comparison of 1-DOF (solid), 2-DOF model (dash-dotted) simulation and experimental ($*$ marks) results for the polynomial spline input.

V. CONCLUSIONS

The optimization framework for designing polynomial splines, as introduced in [2], is used here to design spline inputs for a two Degree-of-Freedom motion system. The optimal spline gives rise to little or no residual vibrations over a wide range of system uncertainty and outperforms two earlier benchmark methods from the literature: the well-known input shaping method [7] and a technique based on Bernstein-Bézier harmonic curves [9].

The optimization of the polynomial spline is a linear program, guaranteeing that the solution is a global optimum that can be found efficiently, in this case within a few CPU seconds. This makes the optimization framework a promising tool for engineers in practice. Moreover, the framework is extremely versatile, allowing to include many different constraints, e.g. boundary constraints, bounds on the input and output and their derivatives, set points on the output, …

VI. ACKNOWLEDGMENTS

REFERENCES

[1] M. Chew and C. H. Chuang, "Minimizing residual vibrations in high-speed cam-follower systems over a range of speeds," *Transactions of the ASME, Journal of Mechanical Design*, Vol. 117, pp. 166–172, 1995.

[2] B. Demeulenaere, J. De Caigny, J. Swevers and J. De Schutter, "Dynamically Compensated and Robust Motion System Inputs Based on Splines: A Linear Programming Approach," *Proc. of the American Control Conference*, New York City, NY, 2007, pp. 5011–5018.

[3] P. Dierckx, *Curve and Surface Fitting with Splines*, Oxford University Press Inc, New York, NY; 1993.

[4] K. Kanzaki and K. Itao, "Polydyne cam mechanisms for typehead positioning," *Journal of Engineering for industry*, Vol. 94 No. 1, pp. 250–254, 1972.

[5] H. Kwakernaak and J. Smit, "Minimum Vibration Cam Profiles," *Journal of Mechanical Engineering Science*, Vol. 10, No. 3, pp. 219–227, 1968.

[6] R. Pintelon and J. Schoukens, *System Identification: A Frequency Domain Approach*, Institute of Electrical and Electronics Engineers, Inc., New York, NY; 2001.

[7] N. C. Singer and W. P. Seering, "Preshaping command inputs to reduce system vibration," *Transactions of the ASME, Journal of Dynamic Systems, Measurement and Control*, Vol. 112, pp. 76–82, 1990.

[8] W. E. Singhose, W. P. Seering and N. C. Singer, "Time-optimal negative input shapers," *Transactions of the ASME, Journal of Dynamic Systems, Measurement and Control*, Vol. 119, pp. 198–205, 1997.

[9] L. N. Srinivasan and Q. J. Ge, "Designing dynamically compensated and robust cam profiles with bernstein-bézier harmonic curves," *Transactions of the ASME, Journal of Mechanical Design*, Vol. 120, pp. 40–45, 1998.